JOURNAL OF OPTOELECTRONICS AND ADVANCED MATERIALS, Vol. 11, No. 9, September 2009, p. 1150 - 1156

On Lagrangian methods in the analysis of piezoelectric resonators and sensors♣

B. DULMET[a*], Y. LAZAROV[b]
[a] *FEMTO-ST, CNRS, Université of Franche Comté, Ecole Nationale Supérieure de Mécanique et des Microtechniques, 26 Chemin de l'Epitaphe 25000 Besançon, France.*
[b] *Institute of Solid State Physics, Bulgarian Academy of Sciences, 72 Tzarigradsko Chaussee Blvd., 1784 Sofia, Bulgaria*

This paper illustrates the use of the so-called Lagrangian method for the modelling of resonant sensors. We put some emphasis on the embedding of the influence of temperature in the analytical modelling of miniature quartz temperature sensors of the strip-resonator type, developed for precise measurement of temperature over wide ranges. The model gives access to the influence of temperature on the frequency and the mode shape of these strip-sensors.

(Received November 5, 2008; accepted December 15, 2008)

Keywords: Lagrangian configuration, Quartz resonators and oscillators, Resonant sensors, Nonlinear acoustics, Dispersive propagation

1. Introduction

Ultra stable oscillators of moderate size and cost still rely on quartz resonators. Such frequency sources provide reliability and robustness even in relatively harsh environmental conditions, although they cannot be considered as primary standards like atomic clocks whose nominal frequency is fixed by the intrinsic properties of the matter, and not by the dimensions of the device. Conversely, it is possible to make piezoelectric resonators sensitive to environmental quantities (temperature, force, acceleration, rotation rate) in a highly selective way. Doing so gives birth to a high-quality class of frequency-output sensors, due to the good resolution granted by the intrinsic frequency stability of the resonator under constant conditions. Nevertheless, a precise analysis of such physical sensors is significantly complicated by thermal effects, whenever the sensor is operated over a large temperature range. Even the basic phenomenon of thermal expansion is poorly addressed in dynamic analyzes provided by standard finite element packages. An excellent method to efficiently embed temperature effects in the analysis of resonant sensors consists of using the Lagrangian configuration, which refers the current state of the studied structure to the known geometry it occupies in a known stress-free reference state. Moreover, establishing the material behaviour laws in the framework of the Lagrangian configuration guarantees that the potential energy be a true scalar, thereby leading to models which are self consistent from the thermodynamic point of view. We present an example illustrating the use of the so-called Lagrangian method to embed thermal effects in the analytical modelling of miniature quartz resonant sensors of the strip-resonator type developed for precision applications.

2. The Lagrangian description of vibrating solids

In most resonant sensors providing a frequency output, the vibration can be described as a small acoustic field superimposed onto a static bias. After the pioneering works of Toupin [1] and Thurston [2] established a consistent theoretical background without much describing its practical application, the use of the Lagrangian configuration to systematically describe the above-mentioned class of problems was developed and successfully applied, for instance by Tiersten and co-workers, to piezoelectric resonator problems with various types of biasing states [3-5]. The starting point of the Lagrangian approach consists of considering the three sets of coordinates which can possibly be used to describe small vibrations superimposed onto a static bias, as shown in Fig. 1.

In this figure, X_L denotes the set of so-called reference coordinates which are defined as the material coordinates

♣ Paper presented at the International School on Condensed Matter Physics, Varna, Bulgaria, September 2008

of the solid at equilibrium, in the absence of both the biasing state and the vibration. We can observe that these coordinates are *fixed* and *known*, which is interesting both from the theoretical and practical points of view. ξ_α represents the set of material coordinates of the solid once the bias is applied and before any vibration exists.

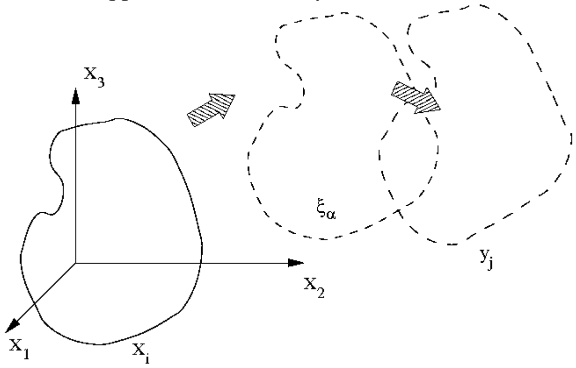

Fig. 1. The three possible sets of coordinates for a quasi-statically biased small vibration.

It is assumed that the bias completely defines the mapping between this intermediate state and the reference state. Finally, one should also define the so-called final or actually time-dependent material coordinates of the vibrating body submitted to a bias. Thus, obviously, for a consistent analysis of problems involving biases like static forces $\boldsymbol{F}$ and/or imposed values of the local temperature θ, one should write:

$$\begin{aligned} y_i &\equiv y_i(\xi_\alpha, t) \\ \xi_\alpha &\equiv \xi_\alpha(X_L, F_L, \theta) \end{aligned} \tag{1}$$

and, consequently, we can consider using various sets of strain gradients for our purposes

$$y_{k,L} \quad \xi_{\alpha,L} \quad X_{M,j} \tag{2}$$

together with the introduction of the acoustic displacement, presumably infinitesimal in the case of linear vibrations:

$$y_j = \left[\xi_\alpha(X_L) + u_\alpha(X_L, t)\right]\delta_{j\alpha} \tag{3}$$

We systematically use the comma notation for a partial derivative, and remark that using different characters for the sets of coordinates guarantees that the formulae are not ambiguous. Also, the convention of an implicit sum over dummy (repeated) indices is systematically used. In counterpart, this approach introduces a frequent need for a Kronecker tensor δ in the expressions. The Kronecker tensor is equal to 1 when its two indices have the same value, and is equal to 0 otherwise.

In this framework, the well–established classical field equations expressing the conservation of linear momentum and electric charge are

$$\begin{aligned} \left(T_{ij}^M + T_{ij}^E\right)_{,i} &= \rho \frac{d^2 y_j}{dt^2} \\ D_{i,i} &= 0 \end{aligned} \tag{4}$$

where $\boldsymbol{D}$ denotes the electric displacement, ρ stands for the mass density in the final state, $\boldsymbol{T^M}$ is the pure mechanical stress tensor and $\boldsymbol{T^E}$ is Maxwell's electrostatic tensor:

$$T_{ij}^E = D_i E_j - \frac{1}{2}\varepsilon_0 E_k E_k \delta_{ij} \tag{5}$$

In addition, $\boldsymbol{E}$ denotes the macroscopic electric field and ε_0 denotes the dielectric permittivity of a vacuum. Thus, one observes that all quantities in Eq. (4) are actually written in terms of the coordinates y_i of the final state. Correspondingly, the essential boundary conditions of an electro-elastic problem should be expressed on the external surface *S* of the body, considered in its final state

$$\begin{aligned} n_i\left[T_{ij}^M + T_{ij}^E\right] &= 0 \\ n_i\left[D_i\right] &= 0 \end{aligned} \tag{6}$$

where brackets are used to denote the jump of a given quantity over the interface and $\boldsymbol{n}$ is the outer normal unit in the final state. There is nothing wrong at this point, but two problems arise when one attempts to solve the problem, especially when the studied structures involve piezoelectric media:

- It has been demonstrated that the condition of rotational invariance of the thermodynamic potential required one to establish the behaviour laws for piezoelectrics, making it necessary to combine the electric field and the deformation gradients along with the finite strain, *i.e.* mixing quantities mapped onto the final coordinates with quantities mapped onto the reference coordinates. Then, the constitutive equations must be established in an intrinsically non-linear theory, whose essentials can be found for instance in [6].
- In the case of biased structures, the exact location of the actual surface *S* may prove to be difficult. Of course, since the so-called linear vibrations are infinitesimally small, we can merge the final and intermediate coordinates in the definition of the surface

$$\delta_{i\alpha} y_i \approx \xi_\alpha \tag{7}$$

Nevertheless, the static deformation arising from the biasing state may be much larger than the acoustic deformation itself. For instance, in conjunction with the anisotropy of thermal expansion in the crystals, the change in the shape of the solid due to temperature variations may seriously impact upon the rigorous treatment of the dynamic problem throughout its boundary conditions, since the classical treatment consists of solving the dynamic problem in terms of the intermediate coordinates.

For instance, in an authoritative work for the determination of the temperature derivatives of the elastic constants of quartz [7] based on resonance measurements of rotated plates of quartz, the changes in the density and thickness of plates with temperature variations were correctly taken into account, but the change in the normal of the anisotropic plate with respect to the internal symmetry axes of quartz was omitted. This omission is mentioned for instance in [5], but it was previously demonstrated in [8] that the resulting error can be easily avoided by using the reference coordinates instead of the intermediate coordinates to map the problem.

The treatment of the electro-elastic problem in terms of the final coordinates y_i is said to be Eulerian. To overcome the fundamental difficulties regarding the derivation of the rotationally invariant constitutive relations (material behaviour laws) briefly described in the first item above, one can use the following field equations in terms of the fixed and known reference coordinates:

$$K^M_{Lj,L} + K^E_{Lj,L} = \rho_0 \frac{d^2 u_\alpha}{dt^2}\delta_{j\alpha} \qquad \Delta_{L,L} = 0 \tag{8}$$

where ρ_0 is mass density in the fixed reference state. These Eqs. must be accompanied by the essential natural boundary conditions on free surfaces delimiting the studied solid structure:

$$n^0_L\left[K^M_{Lj} + K^E_{Lj}\right] = 0 \qquad n^0_L \Delta_{L,L} = 0 \tag{9}$$

Here, one introduces the so-called Piola-Kirchhoff stress tensors $\boldsymbol{K}$ together with the material electric displacement $\boldsymbol{\Delta}$. These quantities are related to the classical quantities through the conservation of elementary surface forces and charges and the changes of variables $X_L \leftrightarrow y_i$:

$$n^0_L K_{Lj} dS_0 = n_i T_{ij} dS = t_j \qquad n^0_L \Delta_L dS_0 = n_j D_j dS = \sigma \tag{10}$$

where t_i denotes the force acting on an elementary surface dS in the final state, corresponding to dS_0 in the unbiased reference state, and σ is the surface charge borne by the same elementary surface. Note that the treatment is the same for the pure mechanical force or for the electrostatic force, so that we did not repeat the formula for $\boldsymbol{K^M}$ and $\boldsymbol{K^E}$. By using chain derivative rules associated with the mapping of Eq. (1), one readily obtains the relations between the tensors of interest:

$$K^{M,E}_{Lj} = J X_{L,i} T^{M,E}_{ij} \qquad \Delta_L = J X_{L,i} D_i \tag{11}$$

where J is the determinant of the Jacobian matrix $[y_{i,L}]$. The treatment of electroelastic problems in terms of the coordinate X_L of the reference state by means of Eqs. (8,9) is said to be Lagrangian. After separating the purely static and the dynamic incremental terms in above equations, it was found that the Lagrangian equations of acoustic fields superimposed on a static mechanical bias can be written in the following form

$$\widetilde{K}_{L\gamma,L} = \rho_0 \ddot{u}_\gamma \qquad \widetilde{\Delta}_{L,L} = 0 \tag{12}$$

where the dynamic incremental Piola-Kirchhoff and material electric displacement tensors can be expanded in the following manner:

$$\widetilde{K}_{Lj} = G^1_{L\gamma M\varepsilon} u_{\xi,M} + G^2_{ML\gamma}\varphi_{,M} \qquad \Delta_L = R^1_{L\gamma M} u_{\gamma,M} + R^2_{LM}\varphi_{,M} \tag{13}$$

Here, $\boldsymbol{G^1}$ and $\boldsymbol{G^2}$ elastic and piezoelectric effective constants are the sums of a bias–dependent and bias–independent terms

$$G^1_{L\gamma M\varepsilon} = c_{L\gamma M\varepsilon} + \hat{c}_{L\gamma M\varepsilon} \qquad G^2_{L\gamma M} = e_{L\gamma M} + \hat{e}_{L\gamma M} \tag{14}$$

Here, $\boldsymbol{c}$ and $\boldsymbol{e}$ are the tensors of the so-called fundamental elastic, piezoelectric and dielectric constants, and the additional terms denoted with a caret ^ depend on the static bias. All necessary formulae are found in Sec.2 of [4]. Due to the small piezoelectric coupling of quartz, piezoelectricity can be omitted in the study of many phenomena in quartz resonators, so we reproduce below only the expression of $\hat{c}$ valid in the absence of any applied static electric field

$$\hat{c}_{L\gamma M\alpha} = T^1_{LM}\delta_{\gamma\alpha} + c^3_{L\gamma M\alpha AB} E^1_{AB} + c_{L\gamma KM} w_{\alpha,K} + c_{LKM\alpha} w_{\gamma,K} \tag{15}$$

$\boldsymbol{T^1}$ is the static stress, $\boldsymbol{E^1}$ is the static strain, and $\boldsymbol{c_3}$ is the tensor of the non linear third order constants, while $w_{a,K}$ represent elements of the tensors of the static strain gradients. This formula is useful in determining the sensitivity of resonators to static forces, but it also shows that the computation of high order sensitivities cannot be practically achieved from fundamental constants, because they would require the measurement of higher order elastic coefficients and their thermal derivatives. Nevertheless, the temperature sensitivity of resonators submitted to transient and non homogeneous temperature variations can be obtained at the first order, with the help of the above equations. When they are used to determine the frequency sensitivity of resonators submitted to static bias of entirely mechanical origin, it is required that all static quantities appearing above are known. In this type of application, the perturbation method described in [4] is a precious tool in the great majority of practical cases, where the biasing states used to achieve frequency-output sensitivity are not homogeneous. Nevertheless, a simple but universally-encountered biasing effect is the thermal expansion, which is stress-free whenever the temperature is uniform and the mounting of the sensor does not preclude its changes in volume. In that simple but useful case, the mapping between the reference and intermediate coordinates can be made explicit, whereas the uniformity of the bias suppresses the need for a perturbation method. Under such circumstances, it becomes quite simple to compute the static temperature sensitivity of a resonator upon a mapping onto the reference coordinates of its structure. This was performed first for the purely elastic case only [8,9], and was extended later to the piezoelectric case [10,11] where appropriate sets of values of the temperature derivatives of the elastic constants of quartz for use in the framework of the Lagrangian configuration were defined and numerical values were computed from resonance measurements from trapped-energy quartz resonators. In this framework, it was shown that the equations of motion in the Lagrangian configuration can be linearized in the following manner [11]

$$\begin{aligned} G_{L\gamma M\varepsilon}u_{\varepsilon,ML} + R_{M\gamma L}\varphi_{,ML} &= \rho_0 \ddot{u}_\alpha \\ R_{L\alpha M}u_{\alpha,ML} - N_{LM}\phi_{,LM} &= 0 \end{aligned} \qquad (16)$$

where the tensors of the *effective* material elastic, piezoelectric and permittivity constants ***G, R, N*** can be measured *directly* as functions of temperature, which avoids the need to link them to the above-mentioned fundamental constants whose determination is practically out of reach for the time being. The effective constants ***G*** and ***R*** exhibit lower symmetries than the classical constants defined in the Linear Piezoelectricity exposures found in textbooks. As a consequence, the elastic constants should be stored in a 9 by 9 matrix instead of a 6 by 6 one. Values for quartz can be found in [11].

3. Temperature sensitivity of high frequency miniature resonant sensors

In the course of a joint research between the laboratories of the two authors, new miniature temperature sensors were developed and realized at ISSP-BAS from narrow quartz plates in NLC-cut operated around 29 MHz [12,13]. It was observed that the compromise between the miniaturization and the stability of these resonant sensors is quite good [14]. We present below an application of the Lagrangian method to the modelling of such miniature sensors, together with the first obtained results.

3.1 Simple bi-dimensional model of strip sensors

The basic design of the sensors is schematically illustrated in Fig. 2. They can be made from $Y+\theta$ singly rotated thin plates of class-32 crystals. In that case, pure shear modes can be driven by an electric field oriented along the normal to the plate. The length of the plate corresponds to the x_3 direction of the rotated plates, according to the IEEE standard definition of $Y+\theta$ singly rotated plates. The mass-loading effect arising from the deposited electrodes confines the acoustic energy in the electroded region. This feature permits one to firmly hold the plates at one or both ends, with practically no loss of acoustic energy, which ensures optimal values of the Q-factor of the resonators. Conversely, there is no such energy trapping effect along x_1, (*i.e.* the width of the resonator) since the electrodes extend over its whole width (schematic configuration).

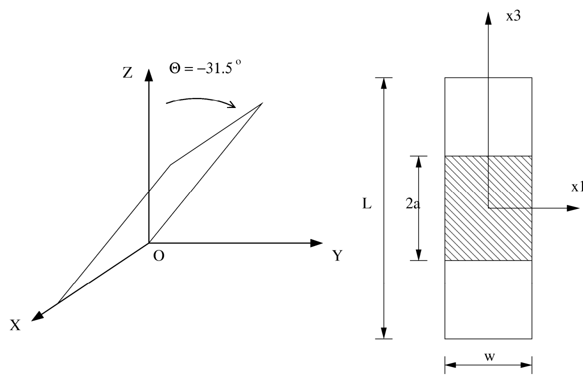

Fig. 2 Schematic design of a strip resonator (top view).

The specifics of the behaviour of such strip resonators already appear in a 2D analysis neglecting the influence of the transverse behaviour along the length of the resonator. Then, the 2D propagation equations pertaining to the purely elastic case and expressed in the Lagrangian configuration, are obtained by substituting $\partial / \partial x_3 \equiv 0$ for all variables in (16) while retaining only the mechanical terms:

$$\begin{aligned} \widetilde{K}_{L\alpha,L} &= \rho_0 \ddot{u}_\alpha \\ \widetilde{K}_{L\alpha} &= G_{L\alpha M\varepsilon}u_{\varepsilon,M} \end{aligned} \qquad (17)$$

with L and M equal to 1 or 2, but not 3, whereas the essential boundary conditions onto free surfaces are

$$G_{L\gamma M\varepsilon}u_{\varepsilon,M} = 0 \, on \quad S_0 \qquad (18)$$

where the effective elastic constants in the Lagrangian configuration are known functions of temperature [11]. More elaborate models of the same 2D problem in the absence of temperature effects were proposed in previous papers [12,13]. Although the model presented here is slightly less accurate from the point of view of acoustics, it enlightens the specific mode couplings at the base of the of strip sensors and it still takes into account more elastic constants than the 3D model of [15], which proposed a unique 3D semi-analytical description of strip resonators in the framework of the widely recognized Mindlin method for the analysis of high frequency vibrations of anisotropic and piezoelectric plates [16,17]. Predicting the temperature sensitivity of strip sensors in the framework of semi-analytical models is still a challenging task.

As a first step, we should determine the solutions of the eigenvalues problem for the pure shear propagation along the thickness of the plate

$$\begin{gathered} G_{2\gamma 2\varepsilon} u_{\varepsilon,22} = \rho_0 \ddot{u}_\alpha \\ G_{2\gamma 2\varepsilon} u_{\varepsilon,2} = 0 \, at \quad x_2 = \pm h \end{gathered} \tag{19}$$

where one takes $2h_0$ as the plate thickness at reference temperature. It is very easy to add correction factors on the essential terms in the model, to approximately account forthe piezoelectric effect, in case of need, so that this issue is left over in this work which concentrates on temperature effects.

Adding the mass loading effect of the electrodes can be easily performed (see [12,13] for instance). The appearance of the value 2 of the indices in (19) comes from the rather standard notation for a quartz resonator where the coordinate x_2 of the working frame is along the thickness of plate. According to the reduced symmetry of the effective constants, we need the G_{99}, G_{22}, G_{44}, G_{29}, G_{49}, G_{24} constants in our notation [11], to describe the general case for plate orientation. For the here–retained type of cut, G_{29} and G_{49} vanish. After normalization, the three eigensolutions u_α^μ are stored in a 3 by 3 square matrix **Q** which is used to define a new set of constants through a linear transformation, in the following manner [18]:

$$\begin{gathered} c^T_{lprm} = Q_{p\gamma} Q_{r\varepsilon} G_{L\gamma M\varepsilon} \\ Q_{i\alpha} = u^\mu_\alpha \delta_{i\mu} \end{gathered} \tag{20}$$

The transformed elastic constants have a different symmetry than the G coefficients. One obtains:

$$c^T_{lprm} \equiv c^T_{mrpl} \tag{21}$$

This variable change projects the mechanical displacement onto the base of pure thickness eigenmodes, which permits one to retain G_{24} and to accurately take into account the linear coupling between the pure thickness shear u_1 and thickness extensional deformation u_2 in the subsequently built model. In the present work, we retained the following terms in the 2D model after the transformation was performed

$$\begin{gathered} c_{11}u_{1,11} + c_{12}u_{2,12} + c_{96}u_{1,22} + c_{66}u_{2,12} = \rho_0 \ddot{u}_1 \\ c_{66}u_{1,21} + c_{69}u_{2,11} + c_{12}u_{1,12} + c_{22}u_{2,22} = \rho_0 \ddot{u}_2 \end{gathered} \tag{22}$$

where we omitted the superscript T denoting the transformed coefficients, to ease the typesetting and readability of the equations. We neglect the coupling between u_3 and the two other components (u_1,u_2) which are the modal components of interest. The natural essential boundary conditions on the major surfaces of the plate are

$$\left.\begin{aligned} c_{12}u_{1,1} + c_{22}u_{2,2} = 0 \\ c_{96}u_{1,2} + c_{66}u_{2,1} = 0 \end{aligned}\right\} at \quad x_2 = \pm h_0 \tag{23}$$

In regions coated with thin metallic electrodes, we should use the following boundary conditions instead

$$\left.\begin{aligned} c_{11}u_{1,1} + c_{12}u_{2,2} = -\rho_0 \omega^2 h_f u_1 \\ c_{66}u_{1,2} + c_{69}u_{2,1} = -\rho_0 \omega^2 h_f u_2 \end{aligned}\right\} at \quad x_2 = \pm h_0 \tag{24}$$

where h_f is the film thickness and h_0 the half thickness of the plate in the reference configuration, which is by definition constant with respect to temperature variations, whereas the transformed elastic coefficients are known functions of temperature. Then one looks for guided waves in the following form

$$\begin{gathered} u_1 = \beta_1 \sin \eta x_2 \cos \xi x_1 \\ u_2 = \beta_2 \cos \eta x_2 \sin \xi x_1 \end{gathered} \tag{25}$$

By substitution into (24) and expressing the need for non–identically null solutions, one obtains an algebraic determinantal equation

$$\begin{aligned} & c_{22}c_{96}\eta^4 + \eta^2 \Big[-\rho\omega^2 (c_{22} + c_{66}) \\ & + \xi^2 \big(c_{96}c_{69} + c_{11}c_{22} - (c_{12} + c_{66})^2 \big) \Big] \\ & + (\rho\omega^2 - c_{11}\xi^2)(\rho\omega^2 - c_{69}\xi^2) = 0 \end{aligned} \tag{26}$$

It has two analytical roots $\eta = f(\xi,\omega)$ which in turn determine two values of the amplitude ratios β_1/β_2. In the most general case, we should look for the solutions as a combination of the two so-called partial waves which are determined in this process. After substitution of that combination into the boundary conditions (23), we obtain a transcendental determinantal equation. Its numerical solution at the current temperature provides the basic dispersion curves presented in Fig. 3 for the case T=25°C. These curves can and must be computed at other temperatures required in the analysis before one can proceed further.

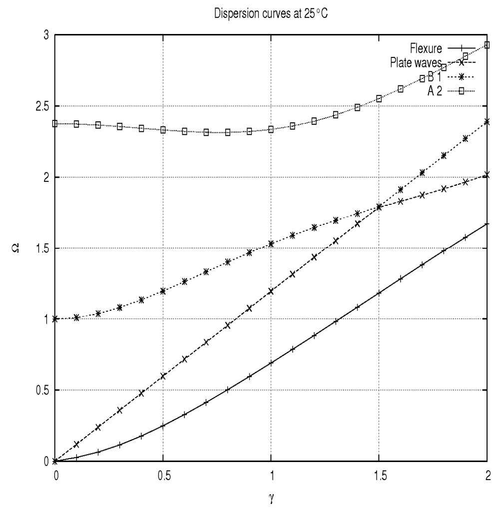

Fig.3. Basic dispersion curves of NLC-cut at 25°C.

This plot was determined after normalizing the angular frequency ω and lateral wave number ξ by their values for the pure thickness case (1D resonances along the vertical axis).

$$\Omega = \frac{\omega}{\omega_0} \quad with \quad {\omega_0}^2 = \frac{c_{96}}{\rho_0}{\eta_0}^2$$
$$\gamma = \frac{\xi}{\eta_0} \quad with \quad \eta_0 = \frac{\pi}{2h_0} \tag{27}$$

In this manner, the dimensionless curves can be used for various designs with different aspect ratios of the narrow plate. The influence of temperature variations on the plot of the dispersion curves is small, so that it is sufficient to present only the curves at 25°C as a typical plot.

In the next step of the method, one considers the most general case of the vibration as a combination of the above–defined branches of the basic dispersion curves. Moreover, it is known that the modes providing good stability as well as electrical output in such plates should have a dominant thickness shear component. In addition, minimum values of the lateral wave number are preferred, since oscillations of the thickness shear displacement component under the electrodes will reduce the generation of electric charges and thereby decrease the motional capacitance and coupling factor of the resonator.

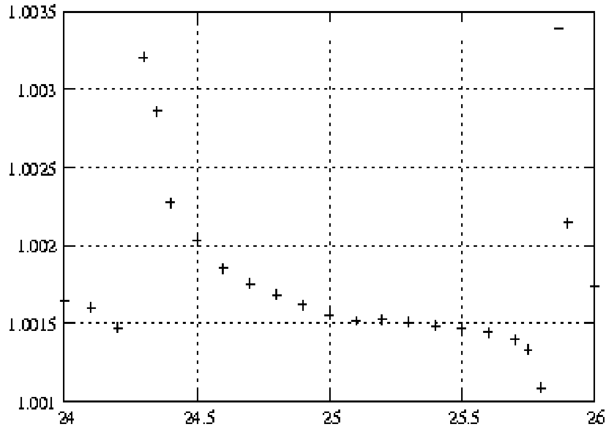

Fig. 4. Dimensionless graph Ω(w/t) for NLC cut strip sensors obtained from the here–presented two-dimensional model

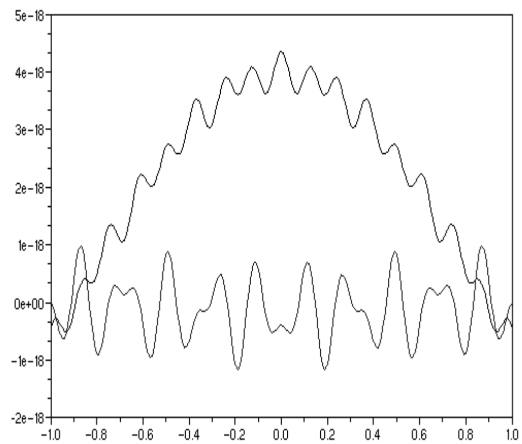

Fig. 5. Amplitude distribution in the cross section at 25°C for w/t=24.5.

The correct conditions can happen in regions of Ω slightly above the horizontal line Ω=1 in Fig. 3. If one restricts the analysis to real values of the wave number γ, (imaginary or complex values will characterize decaying waves that will not carry any energy at all along the plate surface), one observes in Fig. 3 that only three branches must be kept in the combination

$$u_1 = \sum_{m=1}^{3} C^m \cos \xi_m x \sum_{n=1}^{2} \beta_1^{m,n} \sin \eta_m^n x_{21}$$
$$u_2 = \sum_{m=1}^{3} C^m \sin \xi_m x_1 \sum_{n=1}^{2} \beta_2^{m,n} \cos \eta_m^n x_2 \tag{28}$$

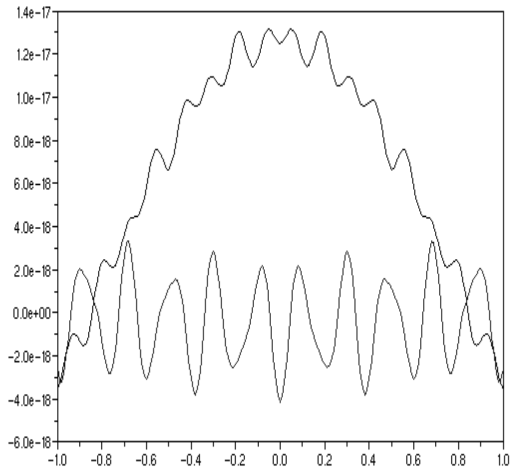

Fig. 6. Amplitude distribution in the cross section at -25°C for w/t=24.5.

From the bottom to the top, these branches are for flexure, plate waves, and essential fast shear in the here–considered cut. Then, the actual 2D model is completed once the balance between the contribution of the three branches is determined together with the resonant frequency, by obeying the edge boundary conditions

$$\left.\begin{array}{l} c_{11}u_{1,1} + c_{12}u_{2,2} = 0 \\ c_{66}u_{1,2} + c_{12}u_{2,2} = 0 \end{array}\right\} at \quad x_1 = \pm\, w/2 \qquad (29)$$

Unfortunately, these boundary conditions cannot rigorously be satisfied by simple combinations of guided waves, so that their influence is approximately taken into account by means of a variational equation derived from Hamilton's principle

$$\int_S K_{11}\delta u_1 + K_{12}\delta u_2 = 0 \qquad (30)$$

where δu_1 and δu_2 denote the variation of solutions arising from an arbitrary change of the C^m constants introduced in (28) to denote the respective weights of each branch into the combination. This leads to a final determinantal equation in terms of either Ω or γ, from which every piece of the model is fixed after a relatively straightforward numerical solution which we shall not discuss here.

3.2 Results and discussion

The model was applied to the computation of the (u_1,u_2) amplitude distributions in the cross–section of NLC-cut strip sensors made at ISSP. We have investigated the ranges of aspect ratio $24 < w/t < 26$ and of temperature $-25°C < \theta < 175°C$. Fig. 4 shows a plot of the dimensionless dispersion curve Ω(w/t) obtained at θ=25°C, and Figs. 5 and 6 show plots of the amplitude distribution at the respective temperatures -25 and +25°C. In the last two figures, one can observe that the amplitude distributions do change with temperature, and from that one is able to predict the noticeable fluctuations of the electrical parameters of the sensors in their operating range, in terms of temperature. The predicted behaviour of the sensors is in qualitative agreement with previous computations by precise FEA and experimental measurement by X–ray topography [12]. Nevertheless, we have found that the aspect ratio *w/t* induced rather small variations of the frequency–temperature characteristic, of the order of a very few ppm/°C. Since the NLC–cut is rather temperature–sensitive, this can be omitted but should be taken care of in the case of temperature–compensated cuts, such as the AT-cut or BT-cut.

4. Conclusions

In this paper, we summarized all required steps of the Lagrangian method to predict the frequency–temperature characteristic of the so–called strip sensors specially designed for thermometric applications. The method is particularly useful whenever the geometry and the crystallographic orientation of the resonators strongly depend on temperature. Nevertheless, other problems also greatly benefit from using the Lagrangian method. For instance, it was successfully used in [13] to compute the force–frequency characteristic of the same kind of temperature sensors. Due to that, it became possible to validate the experiments, despite the presence of temperature fluctuations, since the traction apparatus used for the measurements could not be fully thermo–stabilized. The unified framework provided by the Lagrangian configuration for all sensing purposes relying on the control of some kind of bias is intrinsically a great advantage. This advantage is not defeated by the need for material constants exhibiting lower symmetries than the usual ones, since this reduction of symmetry does not actually add more partial derivatives in the balance equation, in comparison with the classical method. Then, knowing and using the Lagrangian method is mandatory in the study of resonant acoustic sensors, whenever their sensitivity arises from variations of the bias which influence the effective material constants.

References

[1] R. A. Toupin, J. Rational Mech. Anal. **5**, 849 (1956).
[2] R. N. Thurston, "Waves in Solids", in Encyclopedia of Physics, edited by C. Truesdell, Vol. VIa/4, Springer Verlag, Berlin, (1974).
[3] J. C. Baumhauer, H.F. Tiersten, J. Acoust. Soc. Am. **54**, 1017 (1973)
[4] H. F. Tiersten, J. Acoust. Soc. Am. **64,** 832 (1978).
[5] H. F. Tiersten, Electroelastic non linearities, biasing deformation and piezoelectric vibrations in Elastic Waves Propagation, M. F. McCarthy and M. A. Hayes (ed.), Elsevier Science Publisher B. V. [North-Holland), (1989).
[6] H. F. Tiersten, Int. J. Engng. Sci. **9**, 587 (1971).
[7] R. Bechmann, A. D. Ballato, T. J. Lukaszek, Proc. IRE **50**, 1812 (1962).

[8] B. Dulmet, R. Bourquin, C. R. Acad. Sci. Paris **294**, 361 (1982).
[9] B. Dulmet, R. Bourquin, Rev. Phys. Appl. **18**, 619 (1983).
[10] B. Dulmet, R. Bourquin, J. Acoust. Soc. Am. **110**, 1792 (2001).
[11] B. Dulmet, R. Bourquin, E. Bigler, S. Ballandras, J. Acoust. Soc. Am. **110**, 1800 (2001).
[12] B. Dulmet, L. Spassov, R. Bourquin, A. Ivan, Ts. Angelov, Yu. Lazarov, Proc. Eur. Freq. and Time Forum, on CD-ROM, Besançon (2005).
[13] B. Dulmet, P. Tinguy, Yu. Lazarov, L. Spassov, Proc. of joint meeting IEEE Intl. Freq. Ctrl. Symp. and Eur. Freq. and Time Forum, on CD-ROM, Geneva (2007).
[14] L. Spassov, V. Gadjanova, R. Velcheva, B. Dulmet, Proc. IEEE Trans. on UFFC, **55** (7), 1626 (1986).
[15] H. F. Tiersten, T. L. Sham, Proc. IEEE Int. Freq. Ctrl. Symp. **1998**, 947 (1998).
[16] R. D. Mindlin, Quarterly of Applied Mathematics **1**, 51 (1961).
[17] R. D. Mindlin, Intl. J. Solid. Struct. **8**, 895 (1972).
[18] D. S. Stevens, H. F. Tiersten, J. Ac. Soc. Am. **79**, 1811 (1986).

*Corresponding author: bdernard.dulmet@ens2m.fr